

## Pravastatin attenuates carboplatin-induced cardiotoxicity via inhibition of oxidative stress associated apoptosis

Ching-Feng Cheng · Shu-Hui Juan · Jin-Jer Chen ·  
Ying-Chi Chao · His-Hsien Chen · Wei-Shiung Lian ·  
Chun-Yi Lu · Chung-I Chang · Ted-H Chiu ·  
Heng Lin

Published online: 16 May 2008  
© Springer Science+Business Media, LLC 2008

**Abstract** The objective of this study was to evaluate the cardiac toxicity induced by carboplatin, a second generation platinum-containing anti-cancer drug, and to test whether pravastatin can reduce this cardio-toxicity. In the present study, infusion of carboplatin (100 mg/kg) to mice resulted in decreased survival rates and abnormal cardiac histology, concomitant with increased cardiac apoptosis. In addition, treatment of cultured rat cardiomyocytes with carboplatin (100  $\mu$ M for 48 h) caused marked apoptosis and increased caspase-3, -9, and cytochrome C, but decreased BCL-XL protein expression, and this was inhibited by reactive oxygen species (ROS) scavenger *n*-acetylcysteine. Furthermore, pretreatment of cardiomyocytes with pravastatin (20  $\mu$ M) before carboplatin exposure significantly attenuated apoptosis and decreased caspase-3, -9, cytochrome C

activity. Lastly, mice pre-treated with pravastatin before carboplatin treatment showed improved survival rate and cardiac function, with reduced cardiomyocyte apoptosis via activating Akt and restoring normal mitochondrial HAX-1 in heart tissue. In summary, our results show that carboplatin can induce cardiotoxicity in vivo and in cultured cells via a mitochondrial pathway related to ROS production, whereas pravastatin administration can reduce such oxidative stress thus prevented cardiac apoptosis. Therefore, pravastatin can be used as a cytoprotective agent prior to carboplatin chemotherapy.

**Keywords** Carboplatin · Apoptosis · Statin ·  
Reactive oxidative stress · Cardiomyocytes · Cardiotoxicity

Ching-Feng Cheng and Shu-Hui Juan contributed equally to the work.

C.-F. Cheng · T.-H. Chiu · H. Lin (✉)  
Graduate Institute of Pharmacology & Toxicology and College  
of Medicine, Tzu Chi University, 701, Chung Yang Road,  
Section 3, Hualien City, Hualien 970, Taiwan  
e-mail: linheng@ibms.sinica.edu.tw

C.-F. Cheng · W.-S. Lian  
Department of Pediatrics, Tzu Chi General Hospital,  
Taipei Branch, Taipei, Taiwan

C.-F. Cheng · J.-J. Chen · Y.-C. Chao · W.-S. Lian · H. Lin  
Institute of Biomedical Sciences, Academia Sinica,  
Taipei, Taiwan

S.-H. Juan · H.-H. Chen  
Department of Physiology, Taipei Medical University,  
Taipei, Taiwan

C.-Y. Lu · C.-I. Chang  
Department of Pediatrics and Cardiovascular Surgery,  
National Taiwan University Hospital, Taipei, Taiwan

### Introduction

Carboplatin (*cis*-diammine-1,1-cyclobutanedicarboxylate-platinum II), a second generation platinum-containing anti-cancer drug, is currently used clinically against lung, ovarian, head, and neck cancers [1, 2]. Carboplatin is more water-soluble and produces fewer adverse reactions than its analog cisplatin, but its DNA-damaging activity is equivalent to cisplatin at similar toxic doses [3]. The anti-tumor action of carboplatin is mediated by alkylation of DNA followed by cancer cell death. Since carboplatin produces fewer toxic adverse effects than cisplatin, it can be used at higher doses to achieve optimal anti-tumor effects. The predominant dose-limiting toxicities of carboplatin are bone marrow suppression and ototoxicity caused by free radical oxidative injury to these organs [4]. Adverse effects of carboplatin on the heart, although reported, are generally unknown. Cardiac toxicity of carboplatin may be underestimated since it is commonly used with other

chemotherapy with established cardiac toxicity [5]. Carboplatin-induced oxidative stress causes tissue injury [6] and reactive oxygen species (ROS) have been implicated in cardiovascular diseases such as atherosclerosis, hypertension, and heart failure [7]. Therefore, it is reasonable to speculate that carboplatin may result in oxidative stress associated cardiac dysfunction.

Statins, a group of 3-hydroxy-3-methylglutaryl coenzyme A (HMG-CoA) reductase inhibitors, are widely used in clinical practice for their efficacy in reducing plasma cholesterol and in reducing morbidity and mortality in cardiovascular diseases. In addition, statins may also exert significant anti-inflammatory or anti-apoptotic effects on cardiomyocytes [8] and can attenuate heart failure in experimental myocardial infarction mouse models [9]. Although statins can reduce oxidative stress by increasing the bioavailability of nitric oxide, it is unclear whether statins can exert any protective effect against carboplatin-induced cardiac toxicity.

Our present study provides both *in vitro* and *in vivo* evidence that carboplatin can cause cardiac apoptosis by increasing ROS production and administration of statins attenuates apoptosis by reducing oxidative stress. We used pravastatin, one of the commonly prescribed HMG-CoA reductase inhibitors with good water solubility and has been previously applied to rodent experiment [10], to modulate carboplatin-induced cardiac toxicity. We also elucidated the possible molecular mechanisms involved in the cytoprotective effects of pravastatin against carboplatin-induced cardiac toxicity.

## Material and methods

### Animals

Male C57BL/6 mice received humane care in compliance with the Principles of Laboratory Animal Care formulated by the National Society for Medical Research, the *Guide for the Care and Use of Laboratory Animals* prepared by the Institute of Laboratory Animal Resources (NIH publication No. 86-23, revised 1985). The study protocol was approved by the institutional ethics committee on animal research.

### Carboplatin and pravastatin treatment of mice

Carboplatin (Sigma, St. Louis, MO, USA) was dissolved in double-distilled water just before use. Ten weeks old mice were given intra-peritoneal (i.p.) injections of a single dose of carboplatin (50 or 100 mg/kg) on day 1 with (experimental group) or without (control group) i.p. injection of pravastatin (1 mg/kg) on day 0, day 2, and day 4,

respectively. The control group was treated with same volume of normal saline (i.p.) on the day 0, day 2, day 4 instead of pravastatin. All mice were sacrificed on day 6.

### Cardiomyocyte culture

Neonatal cardiomyocytes were isolated and cultured according to the method of Fujio et al. [11] with some modifications. Briefly, the cardiac ventricles of neonatal Wistar rats (1–2 days old) were digested with pancreatin (1.25 mg/ml) at 37°C and cardiomyocytes were isolated and cultured in DMEM containing 10% fetal bovine serum and 0.1 μM bromodeoxyuridine. After 3 days, cells were incubated in serum-free medium containing transferrin (5 μg/ml), insulin (5 μg/ml), and 0.1 μM bromodeoxyuridine for 24 h before treatment with indicated agents.

### Western blot analysis

Cardiomyocytes were lysed in buffer, as previously described [11]. Equal amounts of extracted proteins (50 mg) were separated on SDS-PAGE, transferred to nitrocellulose membranes and probed with primary antibodies. Protein concentrations were determined by the Bio-Rad protein assay. Equal amounts of protein from whole cell lysates (50 μg) were solubilized in 2× SDS sample buffer and separated on SDS-10% polyacrylamide gels as described before [12]. The blots were incubated with antibodies against caspase-3, -8, -9, Bcl-XL, cytochrome C, Akt (1:2,000; Cell Signaling, Beverly, MA), pAkt (1:2,000; Cell Signaling, Beverly, MA), and HAX-1 (1:500; Santa Cruz, California, USA). Blots were washed and incubated with a secondary goat antibody against rabbit IgG conjugated to horseradish peroxidase and exposed to X-ray films. In internal controls, the antibodies were omitted and replaced with β-actin antibody.

### Histopathological preparations and examination

Heart tissue were collected from all groups and were fixed in 4% paraformaldehyde for overnight at 4°C and processed with paraffin wax fixation. Thin sections (5 μm) were then stained with hematoxylin and eosin according to standard protocols.

### Immunohistochemistry

Heart samples ( $n = 6$  for carboplatin treated group and  $n = 6$  for control group) were perfused and postfixed with 4% paraformaldehyde overnight and sectioned (5 μm). After blocking with 30% H<sub>2</sub>O<sub>2</sub> and 5% fetal bovine serum, the sections were then incubated first with polyclonal

anti-cleaved (activated) caspase-3 (1:1,000) antibody for overnight at 4°C and washed three times with wash buffer followed by incubation with horse peroxidase-conjugated goat anti-rabbit IgG (1:50) and developed with DAB.

#### TdT-mediated dUTP-biotin nick labeling (TUNEL) assay and immunofluorescence staining

Mice were perfused with 4% paraformaldehyde in 0.1 M phosphate buffer (pH 7.4). Organs were dissected and postfixed with 4% paraformaldehyde overnight, paraffin embedded and sectioned (5 µm). TUNEL assay was performed according to the manufacturer's protocol (Roche, Mannheim, Germany). Fluorescence immunity hybridization was performed on frozen heart sections (25 µm) using anti-heart specific antibody desmin (1:1,000) and then incubated with anti-dUTP-biotin antibody (1:40) for 1 h at room temperature, washed with PBS and finally mounted with mounting medium containing DAPI (1.5 mg/ml; Vector Labs).

#### Agarose gel electrophoresis for DNA fragmentation

Cells were cultured under the indicated conditions. Attached cells were collected and resuspended in 200 ml PBS containing proteinase K (0.5 mg/ml), RNase A (0.5 mg/ml), and 1% SDS. After 30 min, total lysates were extracted with phenol/chloroform and genomic DNA precipitated with 100% alcohol. Genomic DNA (15 µg) was isotope labeled by klenow enzyme in NEB buffer 2 and  $\alpha$ p<sup>32</sup>dCTP at 37°C for 20 min then klenow activity inactivated at 75°C for 15 min. The labeled genomic DNA was precipitated with phenol/chloroform and 100% alcohol. Finally the genomic DNA fragments were separated on 1.5% agarose gels, dried, and exposed to X-ray film.

#### Measurement of ROS in cardiomyocytes

Production of cellular ROS was evaluated by analyzing changes in fluorescence intensity resulting from oxidation of the intracellular fluoroprobe 5-(6)-chloromethyl-20, 70-dichlorodihydrofluorescein diacetate (CM-H2DCFDA). In brief, cardiomyocytes grown on the coverglass from each treatment group were loaded with 10 µl of the non-fluorescent dye 20, 70-dichlorodihydrofluorescein diacetate (H2DCFDA, Molecular Probes, Eugene, OR, USA) at 37°C for 30 min. The cardiomyocytes were rinsed and the fluorescence intensity was then measured using a fluorescent micro-plate reader at an excitation wavelength of 480 nm and an emission wavelength of 530 nm (Molecular Devices, Sunnyvale, CA, USA). Untreated cells showed no fluorescence and were used to determine background fluorescence, which was subtracted from the treated

samples. The final fluorescent intensity was normalized to the protein content in each group of cardiomyocytes and was expressed as percent of the fluorescent intensity of the control cardiomyocytes.

#### Oxidative fluorescent microtopography

The oxidative fluorescent dye hydroethidine (HE, by Polysciences Inc., Warrington, Germany) was used to evaluate in situ production of superoxide as previously described [13]. HE is freely permeable to cells and in the presence of O<sub>2</sub><sup>-</sup> is oxidized to EtBr, where it is trapped by intercalation with the DNA. EtBr is excited at 488 nm with an emission spectrum of 610 nm. Unfixed frozen heart segments were cut into 30-mm-thick sections and placed on a glass slide and dye HE was topically applied to each tissue section and coverslipped. Slides were incubated in a light-protected humidified chamber at 37°C for 30 min. Images were obtained with a Bio-Rad MRC-1024 laser scanning confocal microscope equipped with a krypton/argon laser.

#### LDH assay

Cytotoxicity was assessed by LDH measurement in the culture medium spectro-photometrically. The LDH release was standardized with a cell injury index defined at  $(A - B) / (C - B) \times 100$ , where A = LDH activity in the test sample; B = LDH activity measured in media without any treatment and C = LDH activity in samples from wells in which cells were lysed with Triton X-100 (100% control).

#### Echocardiography

Mice were anesthetized with phenobarbital (50 mg/kg body weight, i.p.) and measurements were conducted using the Ultrasound Biomicroscopy (UBM) equipment (Vevo 660, VisualSonics Inc., Toronto) with a 30-MHz probe. LV posterior wall thickness, inter-ventricular septum thickness, and LV lumen diameter at both end-systolic and end-diastolic phase were measured digitally on the M-mode tracings and averaged from three cardiac cycles. Fractional shortening was calculated.

#### Statistical analysis

All data are expressed as the means  $\pm$  SEM. The survival analysis was performed using Kaplan–Meier method, and between-group difference in survival rates were tested by the log rank test. Between-group comparisons of the means were performed by one-way ANOVA, followed by *t*-tests. The Bonferroni's correction was done for multiple comparisons of the means.

## Results

Carboplatin treated mice showed decreased survival rate and abnormal cardiac histology due to cardiac apoptosis

The 1 week survival rate of mice in carboplatin (100 mg/kg) treated group was markedly reduced compared to 50 mg/kg carboplatin treated and control groups (Fig. 1a). The histology of hearts from control mice displayed near-normal morphological appearance (Fig. 1b), whereas myofibrils disarray and focal cytoplasmic vacuolization were seen in 100 mg/kg carboplatin treated group (Fig. 1b). In order to examine the degree of apoptosis in heart tissue, TUNEL and DNA fragmentation analysis were performed in the carboplatin (100 mg/kg) injected mice 7 days after the injection. A significant increase (2–5 folds) in TUNEL-positive apoptotic cardiomyocytes was detected in the carboplatin treated group in a dose dependent manner compared to control group (Fig. 2a). Furthermore, TUNEL-positive apoptotic cells were confirmed to be cardiomyocytes because they co-localized with the cardiomyocyte-specific marker, desmin (Fig. 2b). Compatible increments of DNA ladder in a time dependent manner were also found in mice treated with 100 mg/kg carboplatin (Fig. 2c). In addition, immunoblotting with caspase-3 antibody depicted positive results only in the carboplatin-treated mice but not the controls (Fig. 2d).

Carboplatin-stimulated apoptosis is ROS-dependent with caspase activation and can be attenuated by pravastatin

To elucidate whether carboplatin-induced cardiac apoptosis is ROS dependent, primary cultured cardiomyocytes were exposed to different concentrations of carboplatin (100–200  $\mu\text{M}$ ) with or without ROS scavenger NAC, and assayed by DCF immunofluorescence assay. However, to rule out the possibility that pravastatin itself can induce cardiotoxicity, different concentrations of pravastatin (10–200  $\mu\text{M}$ ) were examined for cytotoxicity before the carboplatin-ROS study. Data show that pravastatin had no cytotoxicity to neonatal cardiomyocytes, except at concentrations above 100  $\mu\text{M}$  (Fig. 3a). Carboplatin potently induced ROS production in cultured cardiomyocytes in a concentration-dependent manner and this was inhibited significantly by ROS scavenger, NAC (100  $\mu\text{M}$ ) (Fig. 3b). In addition, carboplatin-induced ROS production and caspase-3 expression can be attenuated by either pravastatin (10–50  $\mu\text{M}$ ) or NAC (100  $\mu\text{M}$ ) (Fig. 3b and c), indicating the mechanism by which pravastatin has a protective effect is similar to NAC. Furthermore, increased expression of apoptotic factors including cytochrome C, caspase-3, and

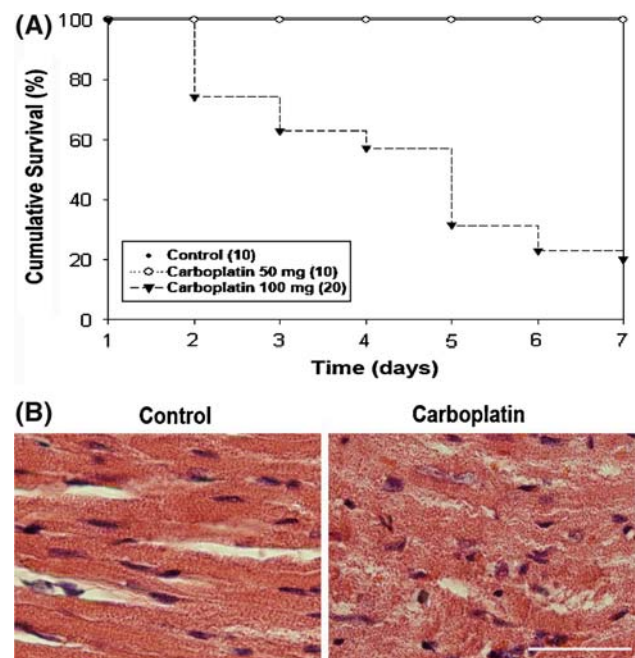


**Fig. 1** Decreased survival rate and abnormal cardiac histopathology in mice treated with carboplatin. (a) Two groups of 10-week-old C57BL/6 mice injected either with carboplatin ( $n = 10$  or  $n = 20$ , with single dose of carboplatin i.p. injection 50 mg/kg or 100 mg/kg, respectively) or with normal saline ( $n = 10$ ) and bred under normal condition for 7 days. Kaplan–Meier survival curves showed decreased survival rate in the 100 mg/kg carboplatin treated mice ( $P < 0.01$ ). (b) Photomicrograph of heart from control mice showing normal histology (left side panel); whereas carboplatin-treated mice (i.p. injection 100 mg/kg) showing myofibril loss and focal cytoplasmic vacuolization in about 15% of cells (right side panel). Heart sections were stained with hematoxylin & eosin as described in material and method section. Bar = 50  $\mu\text{m}$

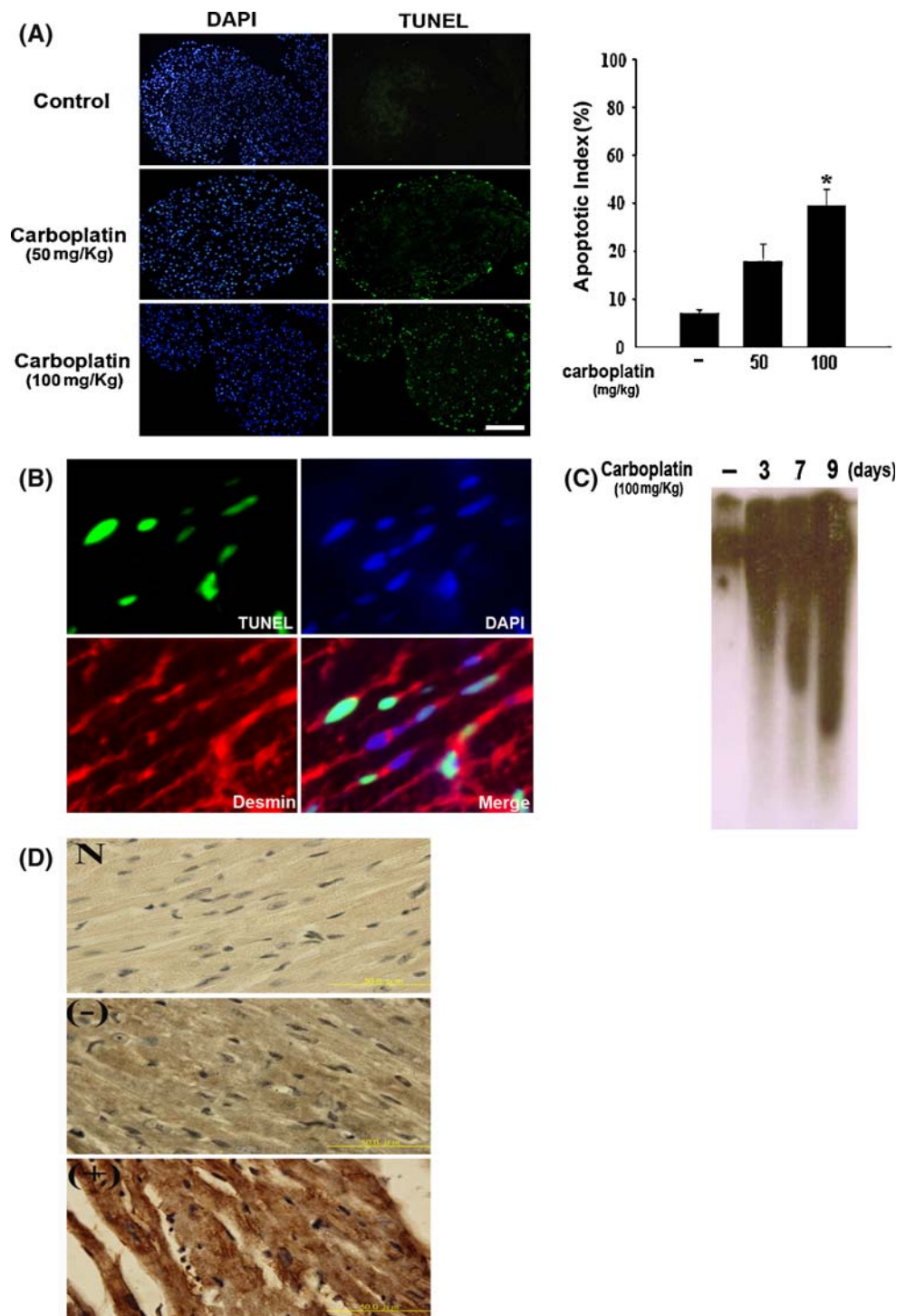
caspase-9, with decreased expression of anti-apoptotic factor BCL/XL were noted in the carboplatin treated cultured cardiomyocytes (Fig. 3d). The expression of these apoptotic factors was attenuated by pre-treatment of neonatal cardiomyocytes with 20  $\mu\text{M}$  pravastatin. Our results show that carboplatin-induced apoptosis is ROS-dependent with caspase activation and can be attenuated by pravastatin.

Pravastatin attenuates carboplatin-induced cardiomyopathy and leukopenia with improved LV function and survival rate in mice

We then evaluated mouse survival rate and in vivo cardiac functions to study the effect of pravastatin on carboplatin-induced cardiotoxicity. Firstly, our Kaplan–Meier analysis revealed that the mice treated with pravastatin in addition to carboplatin (100 mg/kg) showed marked improvement in 7 days survival rate compared to the group treated with carboplatin alone (Fig. 4a). Concomitant TUNEL assay showed a significant decrease in apoptotic cardiomyocytes



**Fig. 2** Apoptosis of cardiomyocytes after carboplatin treatment in mice. (a) C57BL/6 mice were i.p. injected with 100 mg/kg of carboplatin. Apoptotic cardiac myocytes were detected by the TUNEL assay. Left and right panels show the nuclei (blue) and TUNEL positive (green) fluorescence, respectively. Each histogram represents the number of TUNEL-positive cells in carboplatin-treated and control mice from three independent experiments. Bar = 200  $\mu$ m. Quantitative analysis of TUNEL-positive heart nuclei per total nuclei in control and carboplatin treated mice (50 mg/kg or 100 mg/kg, respectively). \* $P < 0.05$ . (b) Colocalization of apoptotic cardiomyocytes stained with TUNEL and cardiomyocytes-specific marker, desmin, and nuclei marker, DAPI. (c) DNA ladder of left ventricular (LV) tissue induced by carboplatin treatment in mice is shown in time dependent manners. (d) Representative photomicrographs of LV sections immuno-blotted with cleaved caspase-3 antibody (1:1,000) for overnight at 4°C followed by incubation with horse peroxidase-conjugated goat anti-rabbit IgG (1:50) for 1 h at room temperature and developed with DAB. Negative controls (N) were performed without anti-caspase-3 antibody. Mice were treated with (+) or without (-) carboplatin (100 mg/kg) before sacrifice ( $n = 5$  animals per group). Bar = 50  $\mu$ m



in the pravastatin + carboplatin treated group compared to the carboplatin only group (Fig. 4b). Secondly, we used echocardiographic study to examine cardiac functions in carboplatin treated mice with or without pravastatin pre-treatment. In agreement with the TUNEL findings, echocardiographic data showed that fractional shortening (FS), inter-ventricular septal thickness (IVS) and LV posterior wall thickness (LVPW) in both diastolic and systolic

phases were significantly thinner in carboplatin-treated than control and pravastatin only (without carboplatin) mice. Normal cardiac contractility and ventricular wall thickness were found to be preserved in the carboplatin + pravastatin treated group (Fig. 5).

In order to elucidate other non-cardiac reasons that might also have an effect on mice survival rate, we examined the blood count parameters at 7 days post

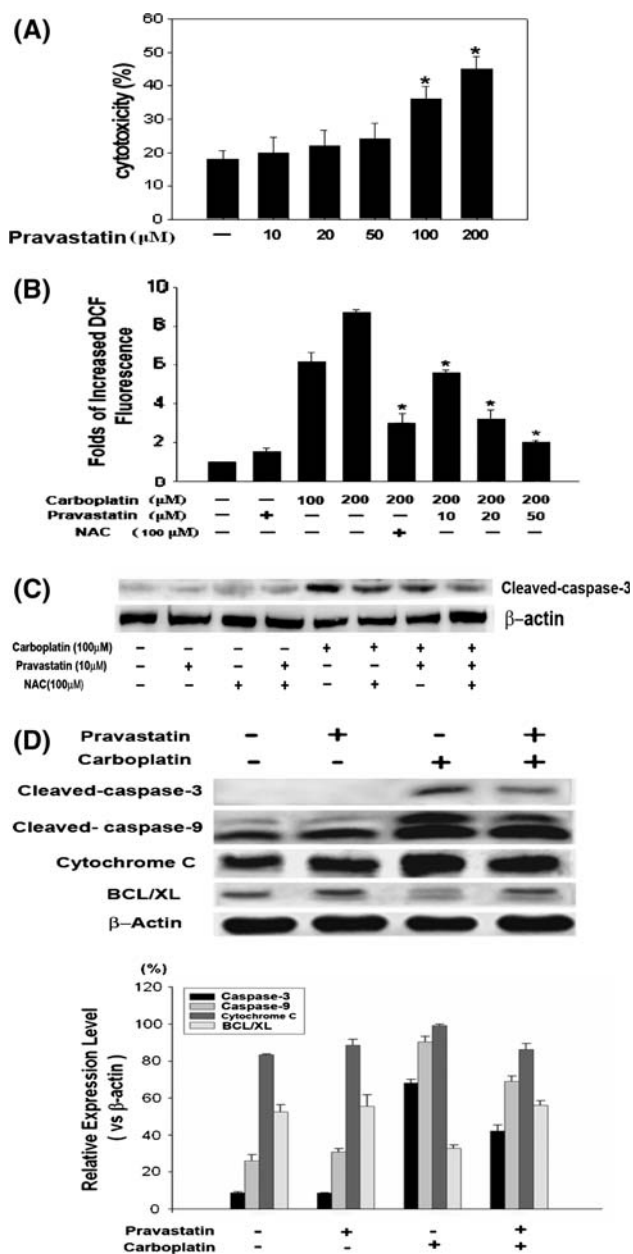


**Fig. 3** Prastatin attenuate ROS production and apoptosis in carboplatin-treated cardiomyocytes. (a) Quantitative cell cytotoxicity was measured by the level of LDH release in cardiomyocytes treated with differential prastatin concentrations from 10 to 200 μM. Bar represents mean ± SD of three experiments separately. (b) Neonatal cardiomyocytes were pre-treated with either prastatin (10–50 μM) or NAC (100 μM) 1 h (h) before the addition of carboplatin (100 or 200 μM), and then incubated for 48 h for ROS quantification. The intracellular ROS concentration was determined by DCF as described in material and methods. \**P* < 0.05 versus control. The protein level of cleaved caspase-3 and β-actin were also measured and shown in (c). (d) Protein levels of caspase-3, caspase-9, BCL-XL, and cytochrome C from cell lysate were assessed by western blotting after 48 h of carboplatin (100 μM) incubation with or without prastatin (20 μM) pre-treatment for 30 min. Data represent results from three independent experiments. Scanning densitometry was used for semi-quantitative analysis in compared to the β-actin levels

**Fig. 4** Improvement of survival rate and attenuation of cell apoptosis follows prastatin treatment in carboplatin-infused mice. (a) C57BL/6 mice were i.p. injected with prastatin 1 day before carboplatin (50 or 100 mg/kg, respectively) treatment. Kaplan–Meier survival curves demonstrated better survival rate (*P* < 0.01) in control group (*n* = 10) and prastatin + carboplatin group (*n* = 16, with survival rate 62%) in comparison with the carboplatin only group (*n* = 18, with survival rate 22%). (b) C57BL/6 mice were i.p. injected with 100 mg/kg of carboplatin with or without prastatin pre-treatment. Apoptotic cardiac myocytes were detected by the TUNEL assay. Left and right panels show the nuclei (blue) and TUNEL positive (green) fluorescence, respectively. Each histogram represents the number of TUNEL-positive cells in carboplatin-treated mice with or without prastatin pre-treatments (*n* = 5 animals in each group). Representative results of three separate experiments are shown. Bar = 200 μm. \**P* < 0.05

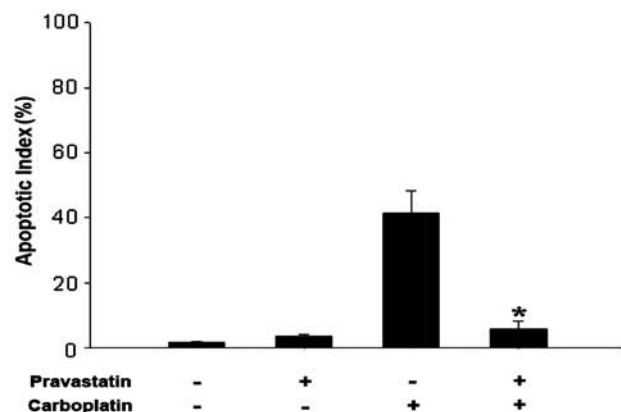
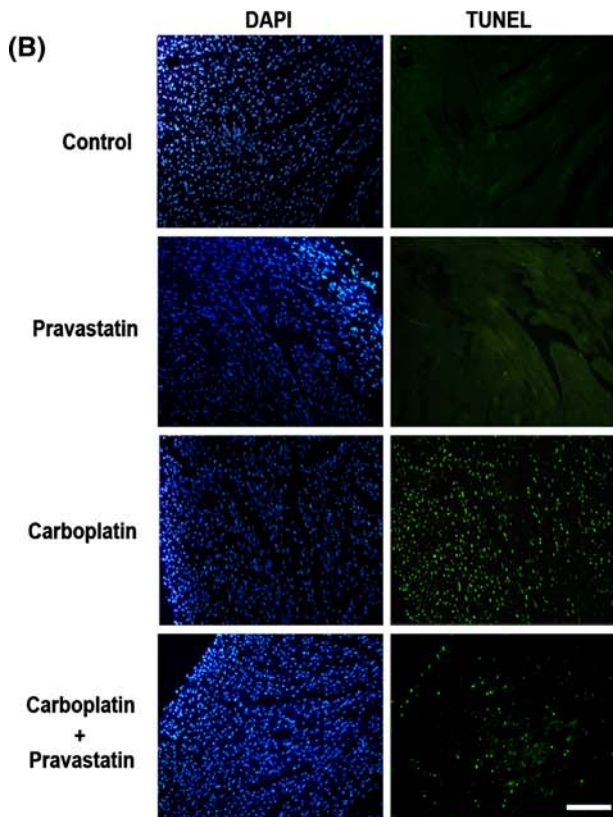
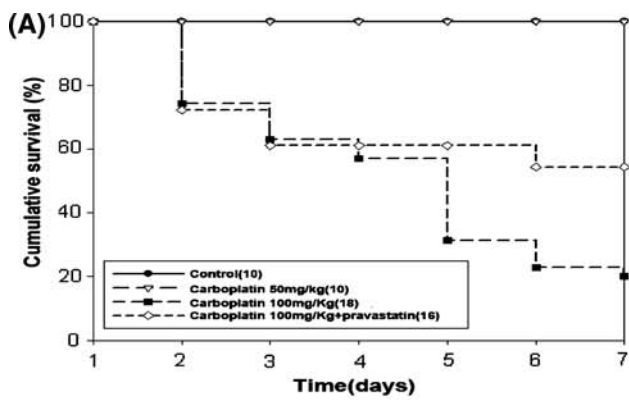
carboplatin treatment. Our result showed that prastatin can partially relieve the bone marrow suppression effect, with prevention of leukopenia (*P* < 0.001), but not the anemia induced by carboplatin treatment (see Table 1). These results correlate with a partial improvement of mice survival rate in prastatin + carboplatin group compared to the carboplatin group (62% vs. 22%).

Prastatin attenuate carboplatin-induced cardiac apoptosis in mice through decrement of caspase and ROS production

Our next in vivo study was intended to detect O<sub>2</sub><sup>-</sup> directly by oxidative fluorescent microtopography. Our data show that carboplatin can induce ROS production in the heart tissue and this can be attenuated by prastatin treatment (Fig. 6a). In concordant to our previous in vitro study, western blotting analysis of heart tissue also showed decrement of caspase-3 activity in the prastatin + carboplatin treated compared to carboplatin alone group. Furthermore, unexpected finding of increase in the level of phosphorylated (i.e. activated) Akt (p-Akt) expression was found in the prastatin + carboplatin group (Fig. 6b).

Prastatin inhibit carboplatin-induced neonatal cardiomyocytes apoptosis via activating Akt and restoring mitochondrial HAX-1

In order to delineate whether the anti-apoptotic effect of prastatin was linked to Akt-PI3 signaling pathway, we conducted the following in vitro studies. Firstly, we demonstrated that prastatin could increase the level of activated Akt (p-Akt) with its peak expression at 12 h post-treatment (Fig. 7a). Secondly, we found that activation of Akt could associate with decrement of caspase-3, implying attenuation of carboplatin-induced apoptosis in cardiomyocytes. These effects were blocked by PI3-kinase inhibitor LY294002 (10 μM), demonstrating that



pravastatin inhibits carboplatin-induced cardiomyocytes apoptosis by activating PI3-kinase dependent pathway (Fig. 7b). In agreement with the western blotting data, the results from TUNEL assay indicated that pre-treatment with PI3-kinase inhibitor LY294002 (10 μM) abolished the therapeutic effect of pravastatin on carboplatin-induced cardiomyocyte apoptosis (Fig. 7c).

Lastly, we explored the possible molecules involved in carboplatin-induced apoptotic cell death, and therefore, the role of a new mitochondria-associated anti-apoptotic protein, the HS-1 associated protein (HAX-1), was examined. Previous data has shown that over-expression of HAX-1 by adenovirus can inhibit hypoxia/reoxygenation-induced cardiomyocytes apoptosis [14]. Accordingly, protein levels of HAX-1 decreased with increasing concentration of cisplatin and related metabolite H<sub>2</sub>O<sub>2</sub> [15]. In the present study we also observed that carboplatin treated cardiomyocyte showed dramatic reduction of HAX-1 levels in mitochondrial fraction without affecting in the cytosolic fraction, with increment of cleaved caspase-3. Such reciprocal changes of mitochondrial HAX-1 and cleaved caspase-3 in carboplatin-treated cardiomyocytes can be prevented by pravastatin supplement (Fig. 7d).

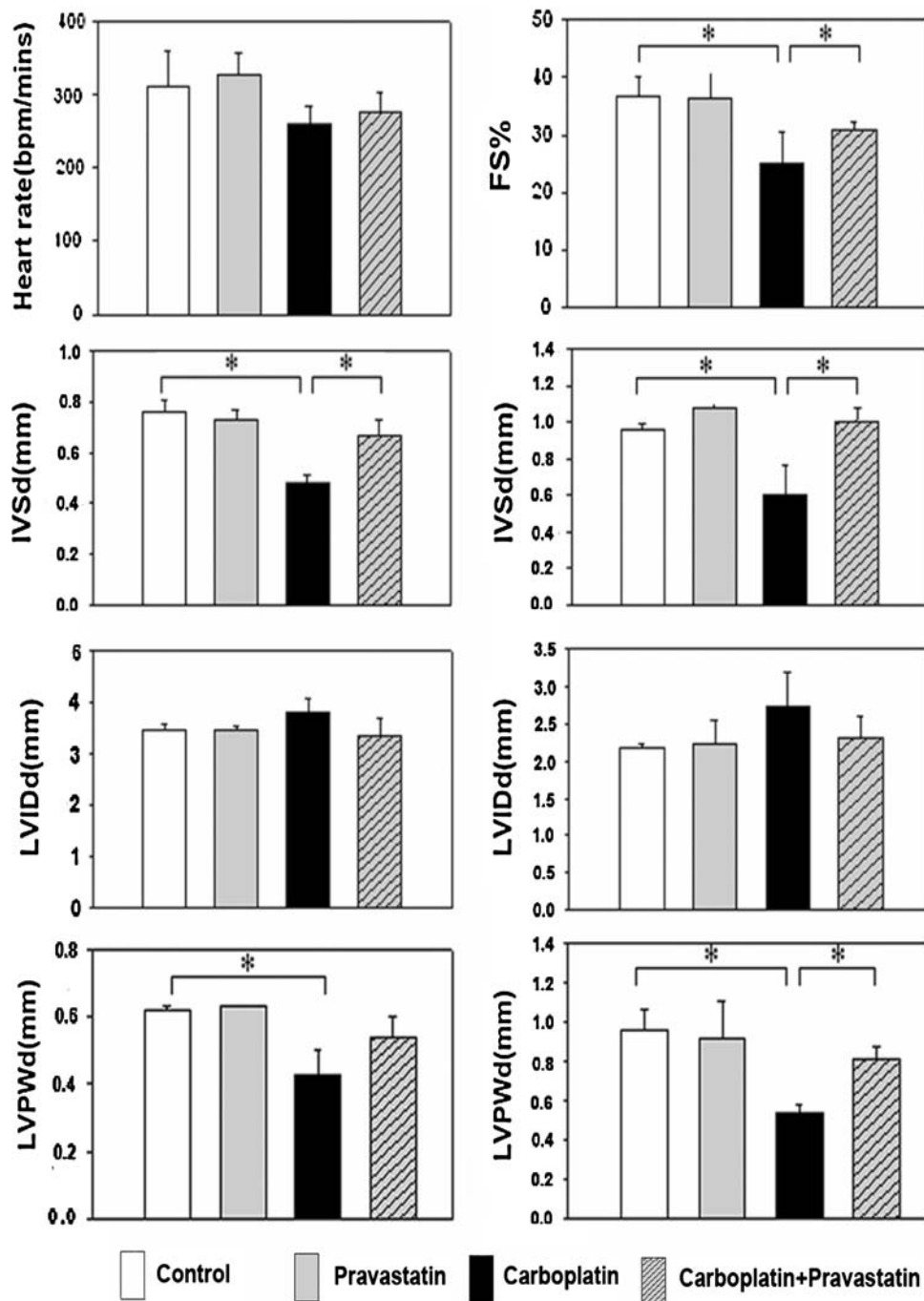
### Discussion

The results of the present study clearly show that carboplatin induced intracellular oxidative stress, activated mitochondria-dependent apoptotic pathway, and stimulated cardiomyocyte apoptosis. We also demonstrated that pravastatin treatment markedly attenuated oxidative stress associated cardiomyocyte apoptosis, concomitant with improved cardiac function and survival rates in mice. The possible mechanism explaining the beneficial effects of pravastatin may involve activating Akt and restoring normal mitochondrial HAX-1 in heart tissue. These results suggest that pravastatin can be used as a cytoprotective agent prior to carboplatin chemotherapy.

Our in vivo study demonstrated that pravastatin therapy completely prevents thinning of the myocardial wall induced by carboplatin. However, we did not observe a concordant improvement in mice survival rates in comparison to the improvement of the left ventricular function (Fig. 5). In fact, only partial rescue of the mice (62%) was found in the pravastatin plus carboplatin group, implying that the heart failure induced by cardiomyocyte apoptosis might not be the major reason for the low survival rate seen in carboplatin treated mice (22%). In fact, carboplatin induced bone marrow suppression with diminution of leukocytes, neutrophils, lymphocytes and erythrocytes with



**Fig. 5** Echocardiographic assessment of cardiac function in mice treated with carboplatin with or without pravastatin supplement. A number of cardiac hemodynamic parameters were assessed 3 days after carboplatin treatment, including T fraction shortening (FS); thickness of inter-ventricular septum at diastole (IVSd) or systole (IVSs); LV internal diameter at diastole (LVIDd) or systole (LVIDs); thickness of LV posterior wall at diastole (LVPWd) or systole (LVPWs). Values are mean  $\pm$  SEM ( $n = 5$  per group). \* $P < 0.05$



subsequent immuno-compromised related infection may be the explanation for high mortality in carboplatin treated mice. Additionally, other side effects of carboplatin such as the cochlear tissue damage has also been reported [16]. Although carboplatin related cardiomyopathy has seldom been reported in clinical conditions, nevertheless, its frequent use in combination with doxorubicin and cyclophosphamide that causes cardiomyopathy [17, 18], warrants us to speculate that the additive effects of this drug combination may damage the cardiac tissue even at

lower accumulative dosage of either drugs. Moreover, we also demonstrated that both carboplatin and doxorubicin exert their effect on cardiac apoptosis through increasing oxidative stress in the heart tissue, and this may strengthen the clinical implications of the present study.

Cardiac apoptosis can be induced through several diverse mechanisms including excessive ROS production or peroxynitrite generation. Increase in ROS production due to doxorubicin chemotherapy regimens can result in cardiomyocyte apoptosis and thus heart failure [19, 20].



**Table 1** Blood count parameters acquired 7 days post-carboplatin treatment in mice

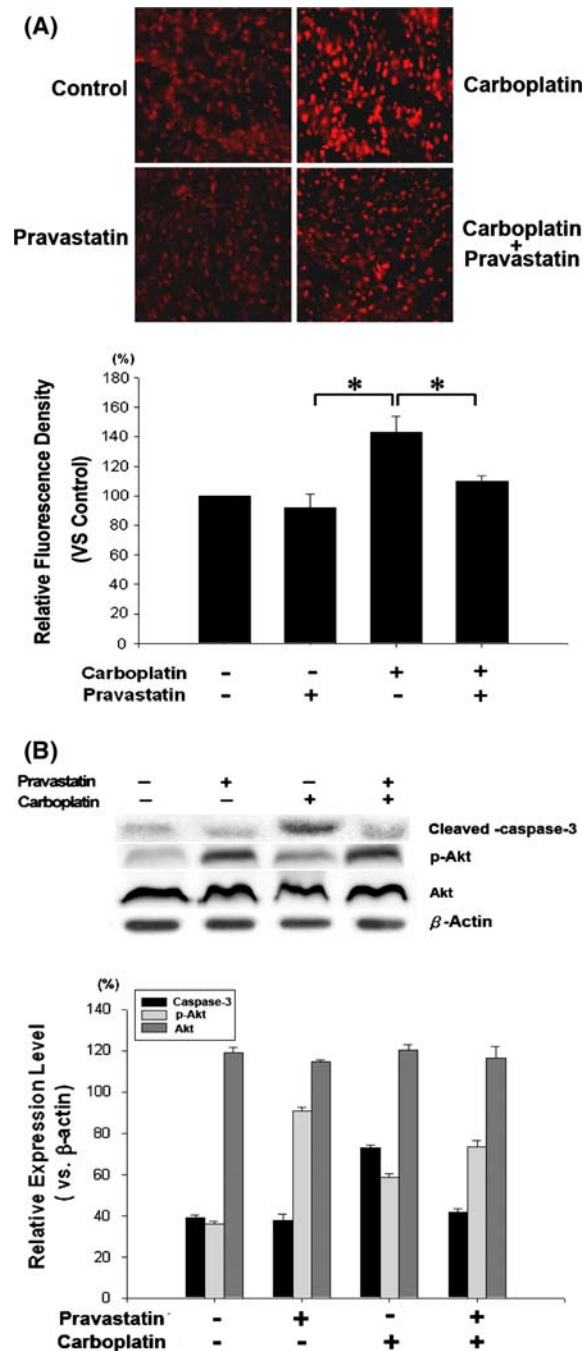
	LEUK ( $10^9/l$ )	ERYTH ( $10^{12}/l$ )	HGB (g/dl)	NEU ( $10^9/l$ )	LYM ( $10^9/l$ )	MONO ( $10^9/l$ )	PLT ( $10^9/l$ )
Control ( $n = 18$ )	$8.17 \pm 2.02$	$8.40 \pm 0.25$	$14.5 \pm 1.88$	$1.96 \pm 1.18$	$4.51 \pm 1.25$	$0.15 \pm 0.07$	$836 \pm 95.3$
CP only ( $n = 7$ )	$1.09 \pm 0.78^{**}$	$6.32 \pm 0.90^{**}$	$9.57 \pm 1.14$	$1.05 \pm 0.7$	$2.77 \pm 2.23^*$	$0.21 \pm 0.18$	$1094 \pm 180^{**}$
CP + St ( $n = 10$ )	$4.52 \pm 1.98^{**\dagger}$	$5.24 \pm 0.72^{**\dagger}$	$8.52 \pm 1.22^{**}$	$1.41 \pm 0.21$	$1.05 \pm 0.84^{**}$	$0.13 \pm 0.12$	$844 \pm 108^\dagger$

CP; carboplatin; CP + St, carboplatin + pravastatin; LEUK, leukocytes; ERYTH, erythrocytes; HGB, hemoglobin; NEU, neutrophil; LYM, lymphocyte; MONO, monocyte; PLT, platelet; \*  $P < 0.05$  compared with control; \*\*  $P < 0.001$  compared with control; \*\*\*  $P < 0.05$  compared with CP only;  $^\dagger P < 0.001$  compared with CP only

Pro-inflammatory cytokine stimulation of both superoxide and NO-generating activities can enhance peroxynitrite production which results in myocardial apoptosis [21]. However, increased NO activity is apparently not involved in carboplatin-induced cardiomyocyte apoptosis since iNOS, TNF- $\alpha$ , IL-6, interleukin-1 $\beta$ , interferon- $\gamma$ , which are sources of NO production, were severely attenuated in the carboplatin-treated cardiomyocytes in our real time PCR assay (data not shown). Accordingly, carboplatin is similar to doxorubicin in augmenting ROS production thus results in cardiomyocyte apoptosis via mitochondria dependent pathway with increased caspase-3, -9, and cytochrome C, but not caspase-8, activation. Besides, by using an alternative oxidative fluorescent microtopography method we showed that carboplatin induced production of  $O_2^-$  can be attenuated by pravastatin. Furthermore, activation of Akt (a downstream target of PI 3-kinase) in pravastatin-infused mice was found to be critical for the prevention of cardiomyocyte death. However, we could not exclude the cytotoxic effect of carboplatin in inducing DNA intra- and interstrand cross-links, which could have also aggravated the observed cardiotoxicity seen in the present study.

Many studies have shown that oxidative stress related cardiotoxicity involves the activation mitochondrial apoptosis pathway, in which caspase-9, but not caspase-8, is the key regulating factor [22]. Several mechanisms, including

**Fig. 6** Pravastatin attenuates carboplatin-induced ROS production and apoptosis via activation of pAkt in mouse heart. (a) Representative fluorescent photomicrographs of confocal microscopic section of heart labeled with oxidative dye HE (red fluorescence when oxidized to EtBr by  $O_2^-$ ). At identical laser and photomultiplier settings, fluorescence in the carboplatin treated heart is markedly increased compared to control group and mice treated with pravastatin alone. Scanning densitometry was used for semi-quantitative analysis compared to control. Heart sections from mid-ventricular region of LV were examined and 3 tissue slices were checked in each mouse heart ( $n = 4$  mice in each group). Each scanning were performed twice for confirmation. \* $P < 0.05$ . (b) C57 BL/6 mice were injected with pravastatin (i.p. 1 mg/kg) 1 day prior to carboplatin (i.p. 100 mg/kg) treatment, and assess for caspase-3, pAkt and Akt expression level via western blotting. \* $P < 0.05$ . Scanning densitometry was used for semi-quantitative analysis compared to  $\beta$ -actin level. Results are representative data from three separate experiments



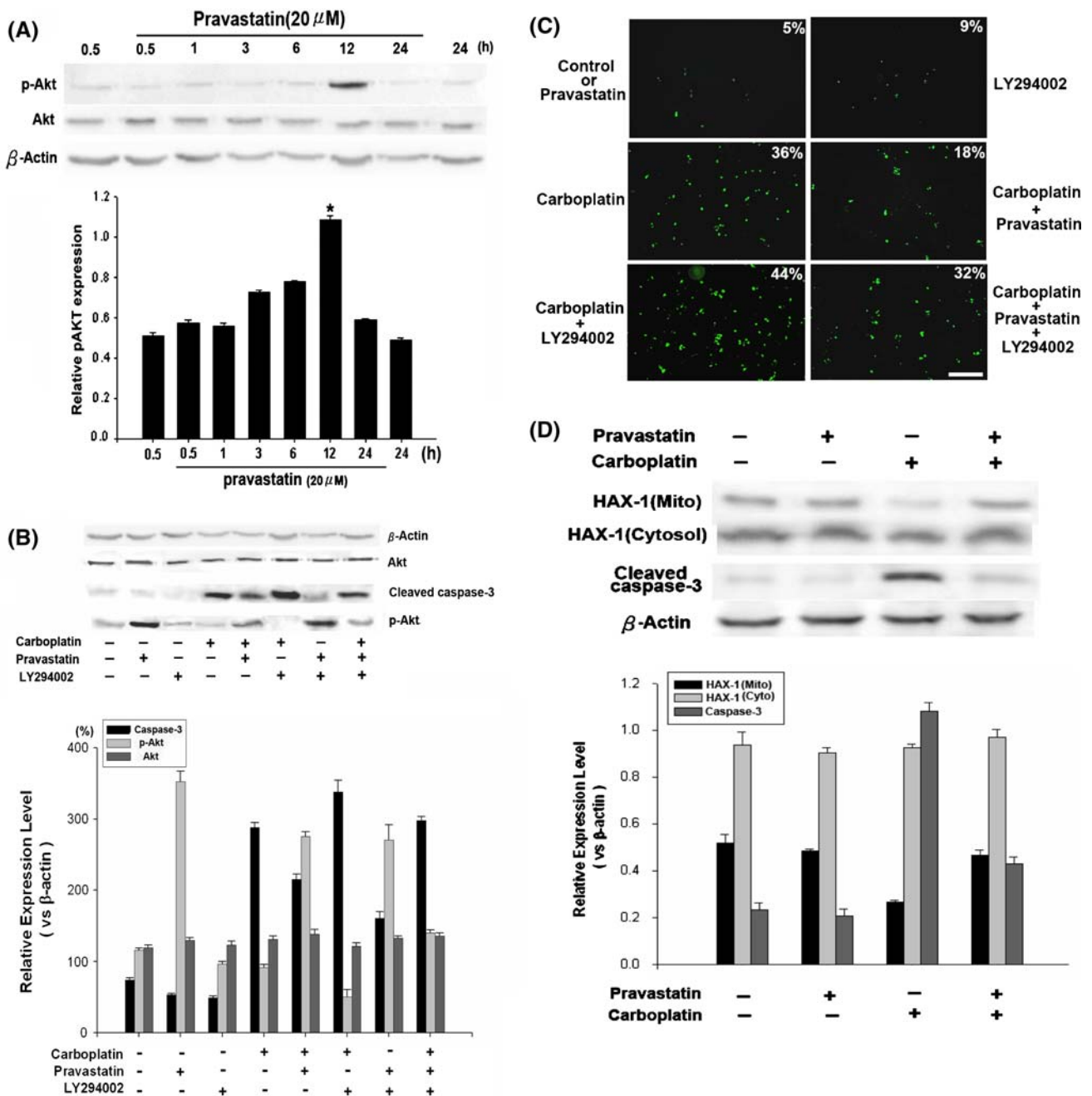


**Fig. 7** Pravastatin inhibits carboplatin-induced apoptosis via activation of Akt and restoring mitochondrial HAX-1 in neonatal cardiomyocytes. **(a)** Time-course analysis of Akt and active form of (phosphorylated) Akt (p-Akt) with 20  $\mu$ M pravastatin treatment in cardiomyocytes. **(b)** Effect of pharmacological inhibition of PI3-kinase (LY294002) on p-Akt and cleaved caspase-3 expression. Cells were pre-treated with pravastatin (20  $\mu$ M) and/or LY294002 for 30 min before addition of carboplatin (200  $\mu$ M). The cell lysate were blotted with cleaved caspase-3, p-Akt and Akt. Scanning densitometry was used for semi-quantitative analysis compared to  $\beta$ -actin level. Results are representative of three separate experiments. **(c)**

HAX-1, are involved in regulating caspase-9 activity [14]. Recently, it has been proposed that HAX-1, identified as a 35-kDa interacting partner with HS-1 and a signal-

TUNEL staining of cardiomyocytes in each experimental group was shown and the data for quantitation of TUNEL-positive heart nuclei per total nuclei (%) in each group was included. **(d)** Protein expression of HAX-1 and cleaved caspase-3. Neonatal cardiomyocytes were pre-incubated with pravastatin (20  $\mu$ M) for 1 h and treated with carboplatin (200  $\mu$ M) for 48 h, then the cell extraction was separated into mitochondria (Mito) and cytosol, respectively, for hybridizing with HAX-1 antibody and cleaved caspase-3 antibody. Scanning densitometry was used for semi-quantitative analysis compared to the  $\beta$ -actin level. Results are representative data of three separate experiments

transduction protein in hematopoietic cells can inhibit the activation of caspase-9 [23]. Our data indicated that carboplatin attenuates mitochondrial distribution of HAX-1

and this can result in apoptosis of the cardiac myocytes. On the other hand, pravastatin may exert its cardiac protective effect by maintaining the mitochondrial expression of HAX-1 (Fig. 7d). Further studies are needed to dissect the biological roles of HAX-1 using either over-expression or gene deletion model.

We followed others in choosing the dosage of carboplatin used in the present study. In prior studies, 120 or 50 mg/kg of carboplatin was used for in vivo i.p. injection to mice [24, 25]. In addition, higher dosage of carboplatin (600 mg/m<sup>2</sup> or 200 mg/kg) was also used to induce bone marrow suppression thus resulting in marked attenuation of the survival rate (20% at day 1 post-treatment) in mice [26]. Moreover, clinical patients were given with intravenous infusion of carboplatin (300–500 mg/m<sup>2</sup>) as a single dose to treat solid tumors. Although the dosage of carboplatin used in the present study (100 mg/kg) is equivalent to 300 mg/m<sup>2</sup> and near the lower range of clinical application, its high mortality may be due to different susceptibility between human and rodent, or the dosage adjustment from mg/m<sup>2</sup> to mg/kg is not ideal in applying to rodent studies thus result in bone marrow suppression.

The protective actions of statins against cardio-, hepato-, and renotoxic effects of anti-cancer drugs including cisplatin and doxorubicin in vivo and in cultured cells has been previously reported [27, 28]. A fairly wide range of dosage of pravastatin (1–30 mg/kg i.p.) has been used in mice for cytoprotective effects with significant TNF- $\alpha$  reduction [29, 30]. However, statins have a promising anti-cancer effect by killing proliferating cells at higher doses. It can potentiate anti-tumor activity when used in combination with other chemotherapy regimens such as doxorubicin or cisplatin in human cancer cell line [31]. Besides, studies of statins in exerting pro-apoptotic effect on human lymphoblasts or rhabdomyosarcoma cells have been described [32, 33]. Our in vitro study also showed similar paradoxical effects and observed that pravastatin at concentration lower than 50  $\mu$ M can protect cardiomyocytes from apoptosis; whereas at concentration higher than 50  $\mu$ M, it can cause cytotoxicity in the cardiac cells (Fig. 3a). In fact, our study is also in agreement with prior reports stating that high concentrations of statin increases apoptosis in endothelial cells, whereas lower concentrations could attenuate hypoxia-induced apoptosis [34]. Most interestingly, even using the same dosage, statins exhibit both anti-tumor activity and cardiac protective effect in some tumor animal models [35].

In summary, our results provide both in vitro and in vivo evidence that carboplatin can induce cardiotoxicity via mitochondria dependent apoptosis pathway related to ROS production, which is prevented by pravastatin via the inhibition of oxidative stress and enhancement of Akt

activation and restoration of mitochondrial HAX-1 in heart tissue. Therefore, pravastatin can be used as a cytoprotective agent prior to carboplatin chemotherapy.

**Acknowledgements** This work was supported by a grant (NSC 94-2314-B-303-009) from National Science Council to C.-F. Cheng. The authors have no competing financial interests to disclose regarding this manuscript.

**Funding** Grant support (NSC 94-2314-B-303-009) from National Science Council, Taiwan to C.-F. Cheng.

## References

1. Fujiwara K, Sakuragi N, Suzuki S et al (2003) First-line intraperitoneal carboplatin-based chemotherapy for 165 patients with epithelial ovarian carcinoma: results of long term follow up. *Gynecol Oncol* 90:637–643
2. Pivot X, Cals L, Cupissol D et al (2001) Phase II trial of a paclitaxel–carboplatin combination in recurrent squamous cell carcinoma of head and neck. *Oncology* 60:66–71
3. Alberts DS (1995) Carboplatin versus cisplatin in ovarian cancer. *Semin Oncol* 22:88–90
4. Husain K, Scott RB, Whitworth C et al (2001) Dose response of carboplatin-induced hearing loss in rats: antioxidant defense system. *Hear Res* 151:71–78
5. Tiersten A, Wo J, Jacobson C et al (2004) Cardiac toxicity observed in association with high-dose cyclophosphamide-based chemotherapy for metastatic breast cancer. *Breast* 13:341–346
6. Husain K, Whitworth C, Hazelrigg S, Rybak L (2003) Carboplatin-induced oxidative injury in rat inferior colliculus. *Int J Toxicol* 22:335–342
7. Dhalla AK, Hill MF, Singal PK (1996) Role of oxidative stress in transition of hypertrophy to heart failure. *J Am Coll Cardiol* 28:506–514
8. Bergmann MW, Rechner C, Freund C et al (2004) Statins inhibit reoxygenation-induced cardiomyocyte apoptosis: role for glycogen synthase kinase 3 $\beta$  and transcription factor  $\beta$ -catenin. *J Mol Cell Cardiol* 37:681–690
9. Hayashidani S, Tsutsui H, Shiomi T et al (2002) Fluvastatin, a 3-hydroxy-3-methylglutaryl coenzyme a reductase inhibitor, attenuates left ventricular remodeling and failure after experimental myocardial infarction. *Circulation* 105:868–873
10. Yao HW, Mao LG, Zhu JP (2006) Protective effects of pravastatin in murine lipopolysaccharide-induced acute lung injury. *Clin Exp Pharmacol Physiol* 33:793–797
11. Fujio Y, Nguyen T, Wencker D et al (2002) Akt promotes survival of cardiomyocytes in vitro and protects against ischemia-reperfusion injury in mouse heart. *Circulation* 101:660–667
12. Lin H, Lin TN, Cheung WM et al (2002) Cyclooxygenase-1 and bicistronic cyclooxygenase-1/prostacyclin synthase gene transfer protect against ischemic cerebral infarction. *Circulation* 105:1962–1969
13. Piech A, Dessy C, Havaux X, Feron O, Balligand JJ (2003) Differential regulation of nitric oxide synthases and their allosteric regulators in heart and vessels of hypertensive rats. *Cardiovasc Res* 57:456–467
14. Han Y, Chen YS, Liu Z et al (2006) Overexpression of HAX-1 protects cardiac myocytes from apoptosis through caspase-9 inhibition. *Circ Res* 99:415–423
15. Vafiadaki E, Sanoudou D, Arvanitis DA et al (2007) Phospholaban interacts with HAX-1, a mitochondrial protein with anti-apoptotic function. *J Mol Biol* 367:65–79

16. Husain K, Whitworth C, Somani SM, Rybak LP (2001) Carboplatin-induced oxidative stress in rat cochlea. *Hear Res* 159:14–22
17. Zver S, Zadnik V, Bunc M, Rogel P, Cernelc P, Kozelj M (2007) Cardiac toxicity of high-dose cyclophosphamide in patients with multiple myeloma undergoing autologous hematopoietic stem cell transplantation. *Int J Hematol* 85:408–414
18. Meinardi MT, van Veldhuisen DJ, Gietema JA et al (2001) Prospective evaluation of early cardiac damage induced by epirubicin-containing adjuvant chemotherapy and locoregional radiotherapy in breast cancer patients. *J Clin Oncol* 19:2746–2753
19. Ide T, Tsutsui H, Kinugawa S et al (1999) Mitochondrial electron transport complex I is a potential source of oxygen free radicals in the failing myocardium. *Circ Res* 85:357–363
20. Spallarossa P, Garibaldi S, Altieri P et al (2004) Carvedilol prevents doxorubicin-induced free radical release and apoptosis in cardiomyocytes in vitro. *J Mol Cell Cardiol* 37:837–846
21. Ferdinandy P, Dhanlaxmi H, Ambrus I et al (2000) Peroxynitrite is a major contributor to cytokine-induced myocardial contractile failure. *Circ Res* 87:241–247
22. Kang PM, Haunstetter A, Aoki H et al (2000) Morphological and molecular characterization of adult cardiomyocyte apoptosis during hypoxia and reoxygenation. *Circ Res* 87:118–125
23. Suzuki Y, Demoliere C, Kitamura D et al (1997) HAX-1, a novel intracellular protein, localized on mitochondria, directly associates with HS1, a substrate of Src family tyrosine kinases. *J Immunol* 158:2736–2744
24. Wang H, Li M, Rinehart JJ, Zhang R (2004) Pretreatment with dexamethasone increases antitumor activity of carboplatin and gemcitabine in mice bearing human cancer xenografts: in vivo activity, pharmacokinetics, and clinical implications for cancer chemotherapy. *Clin Cancer Res* 10:1633–1644
25. Boughattas NA, Levi F, Fournier C et al (1990) Stable circadian mechanisms of toxicity of two platinum analogs (cisplatin and carboplatin) despite repeated dosages in mice. *J Pharmacol Exp Ther* 255:672–679
26. Wang H, Li M, Rinehart JJ, Zhang R (2004) Dexamethasone as a chemoprotectant in cancer chemotherapy: hematoprotective effects and altered pharmacokinetics and tissue distribution of carboplatin and gemcitabine. *Cancer Chemother Pharmacol* 53:459–467
27. Iseri S, Ercan F, Gedik N, Yuksel M, Alican I (2007) Simvastatin attenuates cisplatin-induced kidney and liver damage in rats. *Toxicology* 12:256–264
28. Damrot J, Nubel T, Epe B, Roos WP, Kaina B, Fritz G (2006) Lovastatin protects human endothelial cells from the genotoxic and cytotoxic effects of the anticancer drugs doxorubicin and etoposide. *Br J Pharmacol* 149:988–997
29. Yamato M, Watanabe T, Higuchi K et al (2007) Anti-inflammatory effects of pravastatin on helicobacter pylori-induced gastritis in mice. *Dig Dis Sci* 52:2833–2839
30. Yao HW, Mao LG, Zhu JP (2006) Protective effects of pravastatin in murine lipopolysaccharide-induced acute lung injury. *Clin Exp Pharmacol Physiol* 33:793–797
31. Kozar K, Kaminski R, Legat M et al (2004) Cerivastatin demonstrates enhanced antitumor activity against human breast cancer cell lines when used in combination with doxorubicin or cisplatin. *Int J Oncol* 24:1149–1157
32. Cafforio P, Dammacco F, Gernone A, Silvestris F (2005) Statins activate the mitochondrial pathway of apoptosis in human lymphoblasts and myeloma cells. *Carcinogenesis* 26:883–891
33. Werner M, Sacher J, Hohenegger M (2004) Mutual amplification of apoptosis by statin-induced mitochondrial stress and doxorubicin toxicity in human rhabdomyosarcoma cells. *Br J Pharmacol* 143:715–724
34. Weis M, Heeschen C, Glassford AJ, Cooke JP (2002) Statins have biphasic effects on angiogenesis. *Circulation* 105:739–745
35. Feleszko W, Mlynarczuk I, Bakowiec-Iskra EZ et al (2000) Lovastatin potentiates antitumor activity and attenuates cardiotoxicity of doxorubicin in three tumor models in mice. *Clin Cancer Res* 6:2044–2052